

The effect of optical phase conjugation on inter- and intra-channel nonlinearities in ultrahigh speed transmission systems

Xiaosheng Xiao, Shiming Gao, Yu Tian, He Yan, and Changxi Yang*

State Key Laboratory of Precision Measurement Technology and Instruments, Department of Precision Instruments, Tsinghua University, Beijing 100084, China

ABSTRACT

We demonstrate that all the inter- and intra-channel nonlinear impairments can be eliminated simultaneously by optical phase conjugation (OPC) in a power-symmetry system. However, for practical systems without power-symmetry, it is found that the effects of OPC on various nonlinearities are different in the same link. Even some nonlinearities are suppressed and some are enhanced. Therefore, optimizing the transmission link with OPC to suppress the dominant nonlinearity is demanded. By using 1-km-long highly nonlinear fiber (HNLF) and tuning the pump wavelength near the zero dispersion wavelength of the HNLF, we experimentally generate the phase conjugation of the dispersed ~ 300 fs pulses. OPC with conversion efficiency of about -16 dB and conversion bandwidth of about 38 nm is obtained.

Keywords: Optical Kerr effect, optical phase conjugation (OPC), optical fiber communication, inter-channel nonlinearities, intra-channel nonlinearities, spectral inversion, optical pulse.

1. INTRODUCTION

In ultrahigh speed transmission systems, one of the main impairments is the nonlinear Kerr effect¹, which is categorized to two kinds: inter- and intra-channel nonlinearity. The inter-channel nonlinearity includes inter-channel four-wave mixing (FWM) and inter-channel cross-phase modulation (XPM). The intra-channel nonlinearity includes single pulse self-phase modulation (SPM), intra-channel FWM (IFWM) and intra-channel XPM (IXPM). It has been reported that optical phase conjugation (OPC) can compensate for one of the nonlinear impairments in various systems, such as the SPM of single pulse², inter-channel FWM in wavelength-division-multiplexed (WDM) systems³, IXPM in 100-Gb/s single channel system⁴, and inter-channel XPM in long WDM optical links⁵. Generally, there is more than one nonlinear impairment in transmission systems. Such as in WDM systems, inter-channel FWM and XPM as well as the intra-channel nonlinearities degrade the optical signals. Recently, simultaneous suppression of both SPM and inter-channel XPM by OPC and Raman amplification is shown through numerical simulation⁴, and the reduction of the intra-channel nonlinearities by OPC in pseudolinear transmission is reported⁶. Numerous researches have shown that OPC can suppress one or more nonlinear effects in various optical systems. A question arises naturally: can OPC compensate for all the inter- and intra-channel nonlinear effects simultaneously in the same transmission line?

In Section 2, we demonstrate that OPC can eliminate all the inter- and intra-channel nonlinear impairments simultaneously in the same system with power-symmetry. Afterwards, the case of power-asymmetry transmission systems with OPC is investigated in Section 3. It is found that the effects of OPC on various nonlinearities are different, even inverse, in the same link. We present the underway experiment of ~ 300 -fs pulse OPC in Section 4. Section 5 presents the conclusion.

2. SUPPRESSION OF ALL INTER- AND INTRA-CHANNEL NONLINEAR EFFECTS

In this section, by using a unified method, we demonstrate that for transmission link with power symmetry, OPC can compensate for all the inter- and intra-channel nonlinear effects simultaneously in the same link. First, we show that all the inter- and intra-channel nonlinear effects appearing in transmission system are originated from the Kerr effect of the *total electric field*. Similar to the decomposition of the single pulse SPM, IXPM and IFWM from the Kerr effect in single channel¹, we can separate various inter- and intra-channel nonlinearities in high-bit-rate WDM systems. The total electric

* cxyang@tsinghua.edu.cn; phone 8610-62772824

field can be represented as a sum of individual pulses of all channels, i.e. $A(z, T) = \sum_{n=1}^N A_n(z, T)$, where N is the number of total input signal pulses, and $A_n(z, T)$ is the electric field representing the n -th pulse. Substituting this sum into the nonlinear Schrödinger equation⁷, taking group-velocity dispersion (GVD) and nonlinear Kerr effect into account, we obtain:

$$\sum_{n=1}^N \left\{ \frac{\partial A_n}{\partial z} + \frac{\alpha(z)}{2} A_n + \frac{i\beta_2(z)}{2} \frac{\partial^2 A_n}{\partial T^2} \right\} = i\gamma \sum_{n,m,p=1}^N A_n A_m^* A_p. \quad (1)$$

The right-side term of Eq. (1) represent various nonlinearities: when the pulse represented by A_n , A_m and A_p are in the same channel it describes the intra-channel nonlinearities, otherwise it is inter-channel nonlinearities. For example, if $n=m=p$ it represents single pulse SPM, if $n \neq m=p$ it describes inter- or intra-channel XPM, and if $n \neq m \neq p$ or $n=p \neq m$ it is inter- or intra-channel FWM.

It has been demonstrated that the single pulse SPM caused by Kerr effect can be compensated by OPC in power-symmetry systems², which is valid to arbitrary pulse represented by functions with parameters z and T and also valid to pulse train. In principle, all the inter- and intra-channel nonlinearities resulted from the Kerr effects of *total electric field* $A(z, T)$ can be cancelled simultaneously by OPC in the same transmission link with power-symmetry. This claim will be examined in the following simulations.

Moreover, the modulation instability (MI) effect in transmission link can be interpreted in terms of a FWM process between the amplified spontaneous emission (ASE) noise and the signals, which is phase-matched by SPM⁷. Regarding the ASE noise as an input channel of WDM system, the MI effect can also be suppressed by midway OPC, which has been demonstrated recently⁸.

3. OPC IN PRACTICAL LINKS

OPC can compensate for all the inter- and intra-channel nonlinearities simultaneously, however, it is difficult to construct a power-symmetry transmission link in practice. Even by use of the distributed Raman amplification in the transmission system, the OPC compensation technique is limited by the double Rayleigh backscattering. For the power-asymmetry systems, the compensation effects of OPC on these nonlinearities are ineffective as expected: one of these impairments may be suppressed mostly, whereas others may be eliminated little. Even some might be compensated and some might be enhanced. We present two examples to demonstrate the above claims. The system configuration of the two cases is shown in Fig. 1, which is composed of two spans of fibers with an optical conjugator (combined with an amplifier to compensate for the power loss of OPC and fiber absorption) between the two fibers. This configuration is called scaled translational symmetry link⁹, and the dispersion parameters of the two spans fibers D_1 and D_2 have scaled mirror symmetry with $D_1 L_1 = D_2 L_2$ (if there is no OPC, $D_1 L_1 = -D_2 L_2$), where L_1 and L_2 are the length of the first and the second span fiber, respectively.

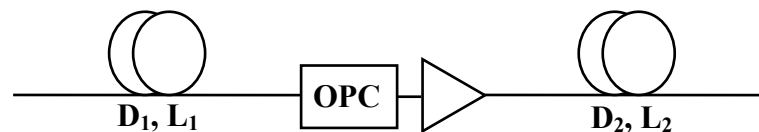


Figure 1: Configuration of the scaled translational symmetry link.

In the first case, a 40 Gb/s nonreturn-to-zero (NRZ) WDM systems is considered. Concentrating on inter-channel FWM and single pulse SPM, spectra of two channels near zero dispersion wavelength are shown in Fig. 2. The main parameters used in the simulations are peak power of pulse $P_0=10$ dBm, $\alpha=0.21$ dB/km, $\gamma=1.5$ km⁻¹/W, the dispersion parameter of the center channel $D_1=0.08$ ps/nm/km, $L_1=L_2=120$ km, and the dispersion-slope of fiber is neglected. The input spectrum is presented in Fig. 2(a) and the output spectra are shown in Figs. 2(b)-(e). Fig. 2(b) corresponds to the power-symmetry system ($\alpha_2 = -\alpha_1$ and without midspan lump amplifier) and without OPC. It can be seen that the spectrum

of the two channels are broadened, which results from single pulse SPM, at the same time two individual frequencies appear at relative frequencies of -80 GHz and 160 GHz due to the inter-channel FWM. The number of FWM-induced frequency components will increase rapidly with the channel number, thus for the general multichannel WDM systems with constant channel spacing, the coherent interference between the FWM-induced frequency components and the signal will degenerate the system performance seriously. In the power-symmetry system with OPC, the output spectrum is presented in Fig. 2(c), which shows that OPC can suppress all the Kerr effects in this case. Considering practical power-asymmetry systems with lump amplifier, the outputs without and with OPC are shown in Figs. 2(d) and (e), respectively. Comparing Fig. 2(e) with Fig. 2(d), we note that OPC suppresses the SPM-induced spectrum broadening. The spectrum broadening of the center channel is reduced to 41%. However, the inter-channel FWM-induced frequency components are enhanced to 8 times at the same time. The enhancement of FWM-induced frequencies by OPC can be explained by the influence of inter-channel XPM on phase mismatch, and the case we considered corresponds to $r > 0.17\pi$ as in Fig. 2 of Ref. [3]. The influence of dispersion slope on the effect of OPC is also investigated. It is found that whether the dispersion slope is compensated or not in the transmission systems, suppressing SPM and enhancing FWM simultaneously by OPC are observed in both cases.

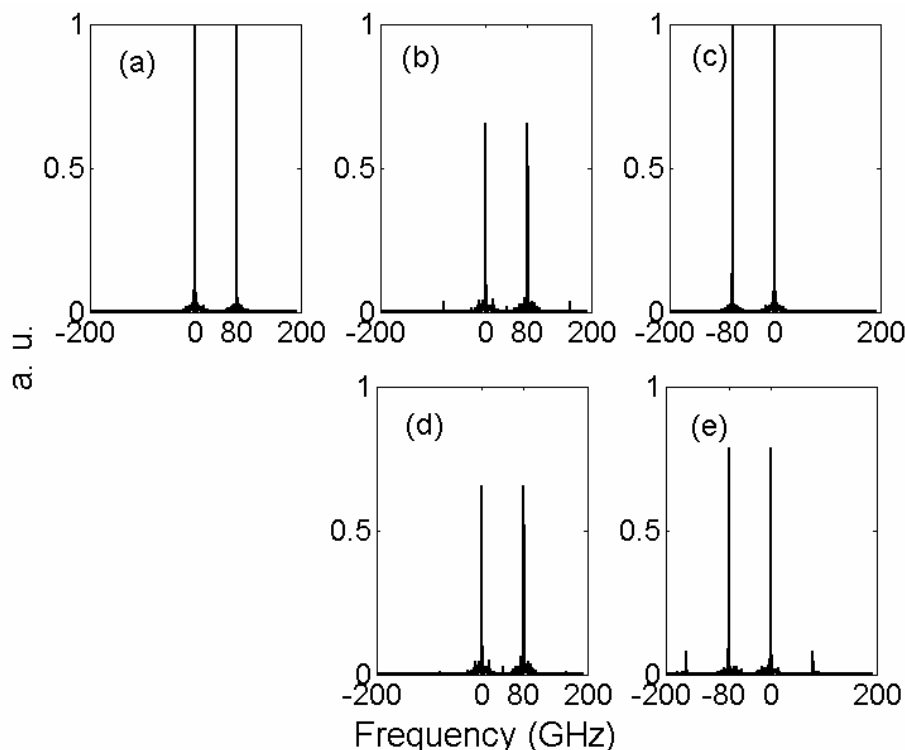


Figure 2: The spectra of two channels in WDM system. (a) Input spectrum. Output spectrum of (b) power-symmetry system without OPC, (c) power-symmetry system with OPC, (d) power-asymmetry system without OPC, (e) power-asymmetry system with OPC.

In the second case we consider high-bit-rate single channel return-to-zero (RZ) system transmitting over the fibers with large dispersion. In order to separate the pulse distortions induced by different intra-channel nonlinearities, an analytical method is adopted^{10,11}. When the signal transmits at rate above 10 Gb/s, the input power is not very high, and the dispersion of the link is fully compensated for, the amplitude of the output field can be represented as $A(L,t)=A(0,t)+A_p(L,t)$, where $A(0,t)$ is the injected signal, and A_p is the perturbations caused by intra-channel nonlinearities. Substituting $A(L,t)$ into Eq. (1), an equation about A_p is obtained which is linear for A_p , thus A_p can be represented by the sum of the contributions given by each single nonlinearity¹⁰. When the input signal is Gaussian-shaped pulse, the analytical expression of A_p caused by each single nonlinearity can be obtained through perturbation theory^{6,10,11}. Considering input Gaussian pulses of which the time separation is T , and assuming no phase coding, single pulse SPM- or

IFWM-induced distortions generated after transmission over the scaled translational symmetry link with (or without) OPC can be described as follows:

$$A_p(L_1 + L_2, t + T_p) = iP_0^{3/2} \exp\left(-\frac{t^2}{6\tau^2}\right) * \int_0^1 \frac{L_2\gamma_2(z)f_2(z) \pm L_1\gamma_1(z)f_1(z)}{\sqrt{1 \pm 2i\xi z + 3\xi^2 z^2}} \exp\left[-\frac{3(2t/3 + T_p - T)^2}{\tau^2(1 \pm 3i\xi z)}\right] dz, \quad (2)$$

where $f(z)$ is the power profile of the link normalized to the input power P_0 ; $\xi=L_1/L_{D1}=L_2/L_{D2}$ is the normalized length and $L_{D1,2}=\tau^2/|\beta_{21,22}|$ is the dispersion length; T_p is the time location of perturbation, τ is the half-width at $1/e$ -intensity point of RZ pulse. When $T_p=T$, Eq. (2) describes the single pulse SPM-induced distortion at the location of the single pulse itself; when $T_p=0$, Eq. (2) represents the IFWM-induced perturbation field which locates at the bit position adjacent to the interacting pulses^{1,11}. If there is a pulse at the time location of IFWM-induced perturbation, we call the perturbation as IFWM@1'bit, otherwise it is IFWM@0'bit. Thus the amplitude jitter of 1'bit in transmission bit sequence is contributed by SPM and IFWM@1'bit, and it is noted that the jitter is caused only by the real part of A_p when all launched pulses are in phase with each other¹². However, the perturbation at 0'bit, resulting from IFWM@0'bit, i.e. ghost pulse, is contributed by not only the real part but also the imaginative part of A_p . When the sign “ \pm ” in Eq. (2) takes “+”, A_p stands for the perturbation filed of the link without OPC and in this case it is represented by A_{p0} , and when “ \pm ” takes “-” A_p stands for the perturbation of the link with OPC and it is represented by A_{pc} . Using reduction ratio $R=1-|\text{Re}\{A_{pc}\}|^2/|\text{Re}\{A_{p0}\}|^2$ to evaluate the compensation for the amplitude jitter of 1'bit caused by SPM or IFWM@1'bit, and $R=1-|A_{pc}|^2/|A_{p0}|^2$ to estimate the suppression of the perturbation of 0'bit caused by IFWM@0'bit, we can judge the effect of OPC on different nonlinear impairments. $R<1$ means that the nonlinear effect is reduced by OPC, i.e. the distortion of the output signal is suppressed and thus the performance of the system is improved. Consider a 40 Gb/s transmission system, with $D_1=16$ ps/nm/km, $L_1=L_2=80$ km, other parameters are the same as Figs. 2(c)-(d). The reduction ratio of SPM, IFWM@1'bit and IFWM@0'bit are 10.3%, 98.6% and 25.0% (also see Fig. 3 at $D_1=16$ ps/nm/km), respectively, which show that the different cancellation of SPM, IFWM@1'bit and @0'bit by OPC are obvious.

Combined with optimal design of transmission link, such as optimizing the dispersion map^{6,13,14}, OPC can cancel nonlinearities greatly. Now we investigate the dependence of the reduction ratio on dispersion map in the case of replacing the first span with DCF and keeping $L_1+L_2=160$ km. Fig. 3 shows the reduction ratio R versus the dispersion parameter of the first fiber D_1 . When D_1 increases, the reduction ratio of SPM varies little, however, that of IFWM@1'bit and @0'bit change with contrary trends. Therefore the optimal dispersion maps for various nonlinearities are different.

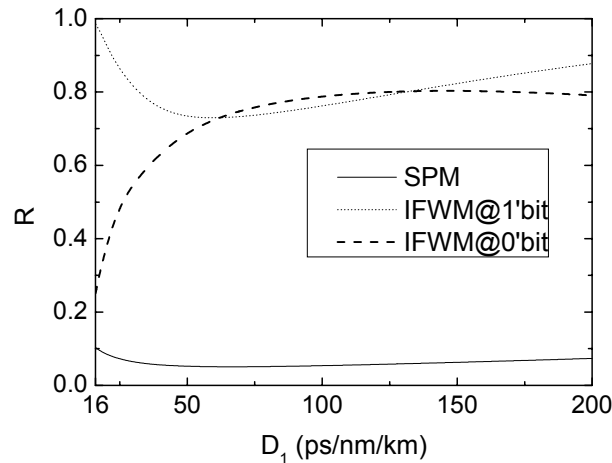


Figure 3: Reduction ratio R dependence of the dispersion parameters of the first fiber D_1 .

Since the effects of OPC on the nonlinear impairments are different in the same transmission system, OPC cannot eliminate all the nonlinear impairments, whereas, one can use OPC to compensate the dominant nonlinear impairment through optimizing the dispersion map or other parameters. In general, one of the nonlinear effects dominates others in a specific system and the main nonlinear effect may be different in other systems^{1,15}. Such as in WDM systems comprised dispersion shift fiber, FWM generated by adjacent channels is the main nonlinear resource. In high-bit-rate NRZ systems, single pulse SPM dominance the nonlinear impairments. For high-bit-rate RZ systems with strong dispersion management, however, IFWM is the dominant impairment¹⁶. Thus for nonlinearity-compensation transmission systems with OPC, optimizing the transmission link is demanded to suppress the main nonlinear resource of this system.

4. FEMTOSECOND PULSE OPC EXPERIMENT

In the past decade, ultrahigh speed transmission experiments, such as 160 Gb/s/Ch and higher bit rates, have been demonstrated^{1,17}. In order to compensate the effect of chromatic fiber dispersion on the ultrashort optical pulse, OPC is one of the most promising techniques because it can not only compensate the even-order dispersion, including the group-velocity dispersion, fourth-order dispersion, and etc., but also suppress the nonlinear Kerr effect. Some groups have investigated short pulse OPC, including ~ps pulse OPC by use of semiconductor optical amplifier (SOA) or highly nonlinear fiber (HNLF)¹⁸⁻²¹, and ~600 fs pulse OPC using LiNbO3 waveguide²². In this section, we introduce the underway experiment of ~300-fs pulse OPC. There are advantages for using HNLF, such as it is compatible with standard telecom components and can be fusion spliced to standard single-mode fiber (SSMF) with low loss. However, ultrashort pulse OPC needs broad conversion bandwidth. In our experiment, the measured bandwidth is broad enough for fs pulse OPC.

The experimental configuration of fs pulse OPC is shown in Fig. 4. The signal pulses are from a passively mode-locked Er-doped fiber laser (FP-LDLS-02 of Calmar Optcom Inc.) and the measured repetition pattern is shown in Fig. 5, which indicates the repetition rate of the output pulses is about 25 MHz. The center wavelength of the fs laser output is tunable and in the experiment it is fixed at 1553.88 nm. Figs. 6(a) and (b) represent the autocorrelation trace and the spectra of the signal pulse. Assuming the waveform of the pulse is sech^2 shape, the full width at half maximum (FWHM) of signal pulse is 255.5-fs. After transmitting through a span of 10-km-long SSMF, the signal pulse broadens extensively in temporal domain, and its spectrum is shown as the dotted curve in Fig. 6(b). Comparing the signal spectra before and after 10-km-long SSMF, it can be inferred that the ultrashort pulse suffers fiber nonlinear effects due to its high peak power. Then the dispersed pulse is combined with an amplified continue wave (CW) pump using a 10:90 coupler. The pump is from a tunable single-frequency laser (Agilent 8164A, wavelength range: 1530-1620 nm) and the pump polarization is adjusted to maximize the OPC efficiency. The pump power after the coupler is about 14 dBm.

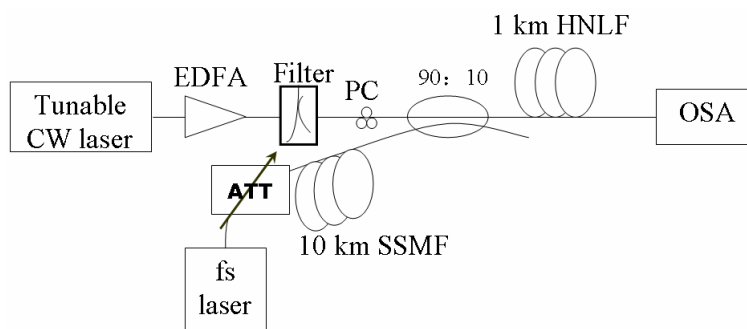


Figure 4: Experimental setup for ~300-fs pulse OPC. ATT: attenuator.

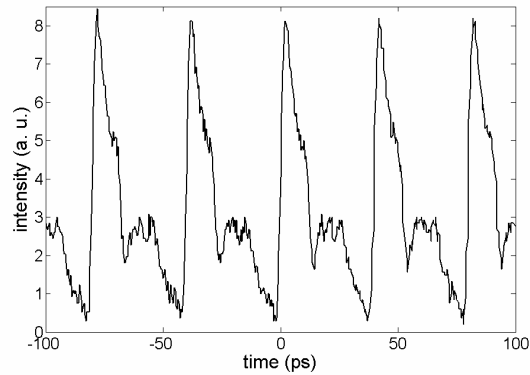


Figure 5: Measured repetition pattern of the fs-laser output.

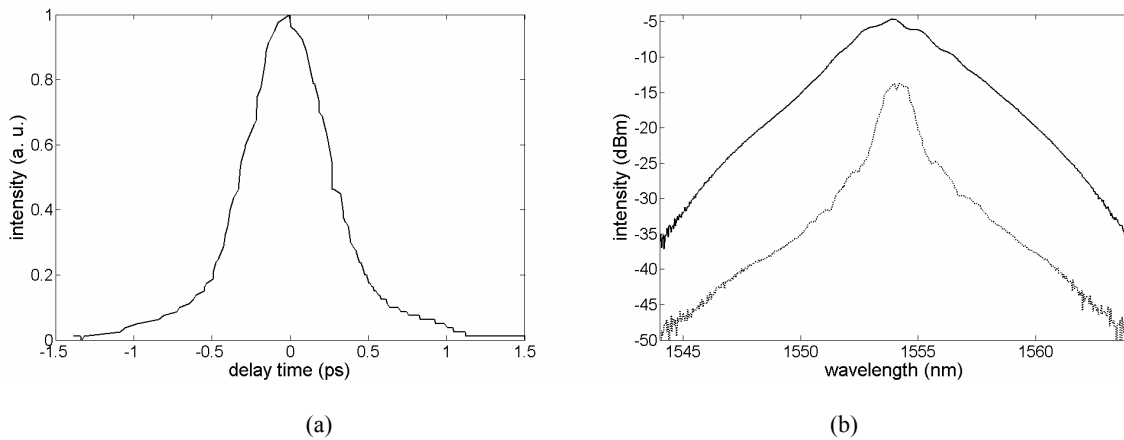


Figure 6: Measured (a) autocorrelation trace and (b) spectra of the signal pulses. The solid curve of (b) is the spectrum of direct output and the dotted curve is the spectrum after transmitted through 10-km-long SSF.

The fs pulse OPC is generated through degenerate FWM process in 1-km-long HNLF. The nonlinear coefficient of the HNLF is about $10.5 \text{ W}^{-1}\text{km}^{-1}$, the zero dispersion wavelength (ZDW) of the HNLF is near 1543 nm, and the dispersion slope at the ZDW is about $0.019 \text{ ps}/(\text{nm}^2\text{km})$. With the HNLF, the FWM efficiencies versus signal wavelength are measured corresponding to different pump wavelengths, as shown in Fig. 7. The measurement setup is the same as Fig. 4 except the signal replaced by a tunable CW laser. When the pump wavelength deviate the ZDW, the 3-dB bandwidth of FWM efficiency is narrow, such as the case of Fig. 7(a). The pump wavelength in Fig. 7(a) is 1554.3 nm where the dispersion is about $0.2 \text{ ps}/(\text{nm km})$, and as shown in this figure, the 3-dB conversion bandwidth is 8.4 nm. However, when the pump wavelength is near the ZDW, the 3-dB bandwidth of FWM efficiency is much wider as $19 \times 2 \text{ nm}$, as shown in Fig. 7(b). Thus with the HNLF and tuning the pump wavelength near the ZDW, we can obtain broad-band FWM or ultrashort pulse OPC.

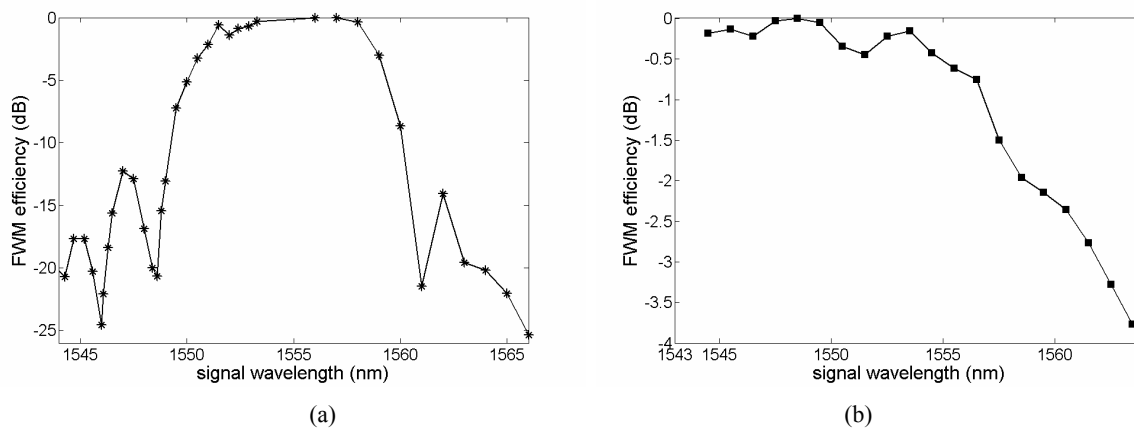


Figure 7: The measured normalized FWM efficiency versus the signal wavelength. The pump wavelength is (a) 1554.3 nm and (b) 1543.0 nm, and the input pump power is kept as 14 dBm.

The spectra of fs pulse OPC output from the HNLF is shown in Fig. 8, where the pump wavelength is 1544.92 nm. In this case, the conversion efficiency, which is defined as the ratio of the output idler power to the input signal power, is -18.3 dB. With the signal fixed, the output idler power versus the pump wavelength is measured as Fig. 9. From Fig. 9 it can be seen that the conversion efficiency reach maximum when the pump wavelength is near the ZDW or the signal wavelength. However, the wavelength of pump near that of signal is not practice for broadband spectral inversion. Therefore, combined with the results of Fig. 7, it is found as expected that choosing the pump wavelength near the ZDW result OPC with maximum conversion efficiency and broadband conversion bandwidth. In this case, the conversion efficiency is -15.95 dB and the 3-dB conversion bandwidth is about 38 nm.

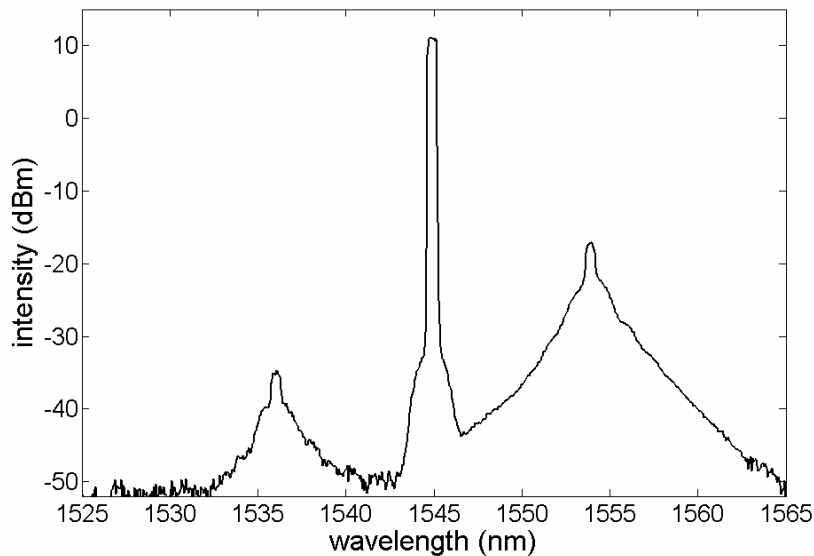


Figure 8: OPC spectra output from HNLF.

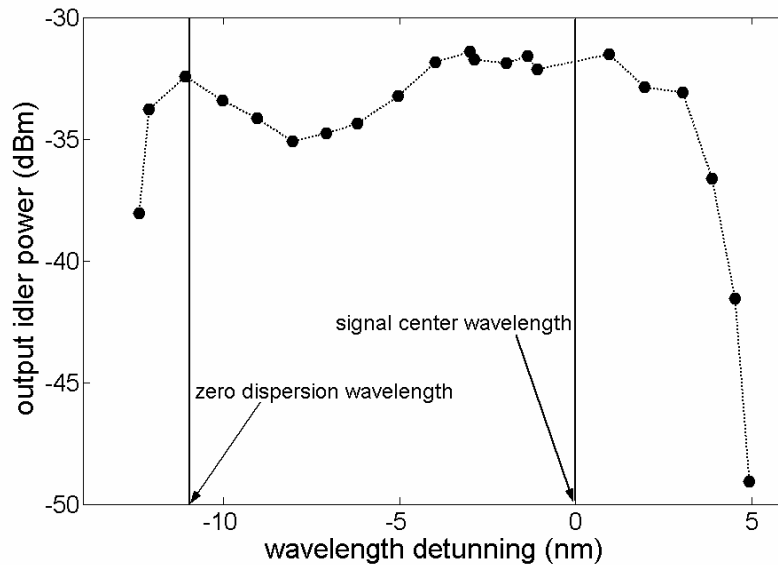


Figure 9: Output idler power measured as a function of the detuning wavelength. The signal is fixed and the pump wavelength varies during the measurement.

For future investigation, in order to investigate the compensation of the dispersion and nonlinear effects on fs pulse by OPC, the output idler would be filtered and transmit through another 10-km-long SSMF. The recovered signal would be compared with the input fs pulse. Besides, using the highly nonlinear photonic crystal fiber (PCF) is under investigation to generate higher conversion efficiency and broader conversion bandwidth.

5. CONCLUSION

Using the unified method, eliminating all the inter- and intra-channel nonlinearities simultaneously by use of OPC has been demonstrated in power-symmetry systems. Then we have presented that, for practical systems, the effects of OPC on various nonlinearities are different, even inverse, in the same link. In general, one of the nonlinear effects dominates the impairments, and for various systems the main nonlinear resource is different. Therefore the optimal design of transmission links with OPC is required to compensate the main nonlinearity. Bu use of 1-km-long HNLf, we experimentally obtained ~300 fs pulse OPC with maximum conversion efficiency about -16 dB and 3-dB conversion bandwidth about 38 nm.

ACKNOWLEDGMENTS

The work is supported in part by the National Natural Science Foundation of China (60478003) and the “Specialized Research Fund for the Doctoral Program of Higher Education” (SRFDP 20040003064).

REFERENCES

1. R.-J. Essiambre, G. Raybon, and B. Mikkelsen, “Pseudo-linear transmission of high-speed TDM signals: 40 and 160 Gb/s,” in *Optical fiber telecommunications IV B*, I. Kaminow and T. Li, eds., Academic, San Diego, Calif., 2002.
2. R. A. Fisher, B. R. Suydam, and D. Yevick, “Optical phase conjugation for time-domain undoing of dispersive self-phase-modulation effects,” *Opt. Lett.* 8, pp. 611-613, 1983.
3. S. Watanabe, “Cancellation of four-wave mixing in a single-mode fiber by midway optical phase conjugation,” *Opt. Lett.* 19, pp. 1308-1310, 1994.
4. I. Brener, B. Mikkelsen, K. Rottwitt, W. Burkett, g. Raybon, J. B. Stark, K. Parameswaran, M. H. Chou, M. M. Fejer, E. E. Chaban, R. Harel, D. L. Philen, and S. Kosinski, “Cancellation of all Kerr nonlinearities in long fiber span using a LiNbO₃ phase conjugator and Raman amplification,” in *OFC2000* 4, pp. 266-268, 2000.

5. G. L. Woods, P. Paparaskewa, M. Shtaif, I. Brener, and D. A. Pitt, "Reduction of cross-phase modulation-induced impairments in long-haul WDM telecommunication systems via spectral inversion," *IEEE Photon. Technol. Lett.* 16, pp. 677-679, 2004.
6. A. Chowdhury and R.-J. Essiambre, "Optical phase conjugation and pseudolinear transmission," *Opt. Lett.* 29, pp. 1105-1107, 2004.
7. G. P. Agrawal, *Nonlinear Fiber Optics*, 3rd ed., CA: Academic, San Diego, 2001.
8. X. Tang and Z. Wu, "Nonlinear noise amplification in optical transmission systems with optical phase conjugation," *J. Lightwave Technol.* 23, pp. 1866-1873, 2005.
9. S. Watanabe and M. Shirasaki, "Exact compensation for both chromatic dispersion and Kerr effect in a transmission fiber using optical phase conjugation," *J. Lightwave Technol.* 14, pp. 243-248, 1996.
10. P. Johansson and D. Anderson, "Generation and dynamics of ghost pulses in strongly dispersion-managed fiber-optic communication systems," *Opt. Lett.* 26, pp. 1227-1229, 2001.
11. A. Mecozzi, C. B. Clausen, and M. Shtaif, "Analysis of intrachannel nonlinear effects in highly dispersed optical pulse transmission," *IEEE Photon. Technol. Lett.* 12, pp. 392-394, 2000.
12. A. Mecozzi, C. B. Clausen, M. Shtaif, S.-G. Park, and A. H. Gnauck, "Cancellation of timing and amplitude jitter in symmetric links using highly dispersed pulses," *IEEE Photon. Technol. Lett.* 13, pp. 445-447, 2001.
13. H. Wei and D. V. Plant, "Simultaneous nonlinearity suppression and wide-band dispersion compensation using optical phase conjugation," *Opt. Express* 12, pp. 1938-1958, 2004.
14. X. Tang and Z. Wu, "Suppressing modulation instability in midway optical phase conjugation systems by using dispersion compensation," *IEEE Photon. Technol. Lett.* 17, pp. 926-928, 2005.
15. R. I. Killey, V. Mikhailov, S. Appathurai, and P. Bayvel, "Investigation of nonlinear distortion in 40-Gb/s transmission with higher order mode fiber dispersion compensators," *J. Lightwave Technol.* 20, pp. 2282-2289, 2002.
16. P. V. Mamyshev and N. A. Mamysheva, "Pulse-overlapped dispersion-managed data transmission and intrachannel four-wave mixing," *Opt. Lett.* 24, pp. 1454-1456, 1999.
17. I. Brener, B. Mikkelsen, G. Raybon, R. Harel, K. Parameswaran, J. R. Kurz, and M. M. Fejer, "160 Gbit/s wavelength shifting and phase conjugation using periodically poled LiNbO₃ waveguide parametric converter," *Electron. Lett.* 36, pp. 1788-1790, 2000.
18. R. I. Laming, D. J. Richardson, D. Taverner, and D. N. Payne, "Transmission of 6 ps linear pulses over 50 km of standard fiber using midpoint spectral inversion to eliminate dispersion," *IEEE J. Select. Topics in Quantum Electron.* 3, pp. 2114-2119, 1994.
19. K. Kikuchi and K. Matsuura, "Transmission of 2-ps optical pulses at 1550 nm over 40-km standard fiber using midspan optical phase conjugation in semiconductor optical amplifiers," *IEEE Photon. Technol. Lett.* 10, pp. 1410-1412, 1998.
20. H. Zheng, S. Xie, M. Chen, M. Yao, and B. Zhou, "Transmission of 12-ps RZ code over 203-km dispersive fiber using mid-span spectral inversion," in *CLEO/Pacific Rim '99*, pp. 487-488, 1999.
21. H. C. Lim, F. Futami, K. Taira, and K. Kikuchi, "Broad-band mid-span spectral inversion without wavelength shift of 1.7-ps optical pulses using a highly nonlinear fiber Sagnac interferometer," *IEEE Photon. Technol. Lett.* 11, pp. 1405-1407, 1999.
22. D. Kunimatsu, C. Q. Xu, M. D. Pelusi, X. Wang, K. Kikuchi, H. Ito, and A. Suzuki, "Subpicosecond pulse transmission over 144 km using midway optical phase conjugation via a cascaded second-order process in a LiNbO₃ waveguide," *IEEE Photon. Technol. Lett.* 12, pp. 1621-1623, 2000.